SUPPLEMENTARY APPENDIX

Energy metabolism is co-determined by genetic variants in chronic lymphocytic leukemia and influences drug sensitivity

Junyan Lu,[1*] Martin Böttcher,[2*] Tatjana Walther,[3] Dimitrios Mougiakakos,[2] Thorsten Zenz[3,4] and Wolfgang Huber[1]

[1]European Molecular Biology Laboratory (EMBL), Heidelberg, Germany; [2]Department of Internal Medicine 5, Hematology and Oncology, University of Erlangen-Nuremberg, Erlangen, Germany; [3]Molecular Therapy in Hematology and Oncology, National Center for Tumor Diseases and German Cancer Research Centre, Heidelberg, Germany and [4]Department of Medical Oncology and Hematology, University Hospital Zürich and University of Zürich, Zürich, Switzerland

**JL and MB contributed equally to this work.*

 doi:10.3324/haematol.2018.203067

Received: July 30, 2018.

Accepted: February 14, 2019.

Pre-published: February 21, 2019.

Correspondence: *WOLFGANG HUBER* -wolfgang.huber@embl.de

THORSTEN ZENZ - thorsten.zenz@usz.ch

DIMITRIOS MOUGIAKAKOS - dimitrios.mougiakakos@uk-erlangen.de

Energy metabolism is co-determined by genetic variants in chronic lymphocytic leukemia and influences drug sensitivity

(Supplementary Materials)

1 Supplementary Methods

1.1 Experimental details for extracellular flux assays

Seahorse XFe96 culture plates (Agilent/Seahorse Bioscience) were prepared by coating each well with Corning™ Cell-Tak Cell and Tissue Adhesive (BD, 354241) according to the manufacturer's recommendations. Additionally, a Seahorse XFe96 cartridge (Agilent, Seahorse Bioscience) was loaded with 200 µl Calibrant solution (Agilent, Seahorse Bioscience) per well and incubated overnight in a CO_2-free atmosphere. The next day, healthy donor-derived, magnetic-bead isolated B cells or CLL peripheral blood mononuclear cells (PBMCs) were thawed from cryo-frozen aliquots, washed in assay specific medium according to the manufacturer's recommendations, and viable cells were automatically counted on a Muse®Cell Analyzer (Merck Millipore). Cells were seeded at a density of 2.4×10^5 cells in 175 µl medium per well. Samples were run with 2-7 technical replicates depending on the material's availability. The ports of the Seahorse cartridge were loaded with 25 µl of each 80 mM glucose, 9 µM oligomycin and 1M 2DG for the glycolysis stress test (GST) and 20 µl of 10 µM oligomycin, 22 µl of 15 µM FCCP and 25 µl of 30 µM antimycin A/rotenone for the mitochondrial stress test (MST). After sensor calibration, assays were run as prescribed in the manufacturer's manual to record ECAR (extracellular acidification rate) and OCR (oxygen consumption rate) over time.

1.2 Quality control criteria for extracellular flux assay measurements

First, we filtered out failed measurements in MST and GST by examining the changes of OCR and ECAR values after compound application, as follows. In MST, there are four stages, and each stage is separated by the application of tool compounds. Based on the biology of mitochondrial respiration, the following criteria were defined (see Supplementary Figure S1 for illustration): the OCR values of stage 2 (after oligomycin and before FCCP injection) should be lower than the OCR values of stage 1 (before oligomycin injection); the OCR values of stage 3 (after FCCP and before rotenone & antimycin A injection) should be higher or equal to the OCR values from stage 1; the OCR values of stage 4 (after rotenone & antimycin A injection) should be lower than the OCR values from stage 1. Similarly, in GST, there are also four stages: the ECAR values of stage 2 (after glucose and before oligomycin injection) should be higher than the ECAR values of stage 1 (before glucose injection); the ECAR values of stage 3 (after oligomycin and before 2-DG injection) should be higher or equal to the ECAR values in stage 2; the ECAR values of stage 4 (after 2-DG injection) should be lower than those in stage 2. Measurements that did not meet these criteria were considered invalid and set aside.

Next, outlier samples were identified based on the modified Z-score of the OCR and ECAR values; the modified Z-score (Z_i) of a measurement point was defined as $Z_i = 0.6745 \times (x_i - \tilde{x})/\text{MAD}$, with $\tilde{x}$ denoting the median of the values from a certain measurement point across all samples and MAD the median absolute deviation. If a certain sample contained more than 40% measurements with modified Z-score higher than 3.5, this sample was considered as an outlier sample and excluded from the subsequent analysis.

Due to the large number of samples, MST and GST were performed over periods of 18 and 16 days, respectively. Therefore, each day was defined as a batch, and batch effects were estimated and adjusted. Specifically, to test for associations between bioenergetic features and categorical variables, i.e., the genomic variants and cell types (B cell VS CLL cell), ANOVA test by including batch as a blocking factor was used. For associations with continuous variables (i.e., drug responses and gene expressions) the batch effect in bioenergetic features was firstly adjusted by using the comBat function in the sva package [1] and then the Pearson correlation test was used.

After the quality control process described above, totally 12 out of 152 samples that did not pass quality control were excluded from subsequent analysis.

1.3 Summarizing bioenergetic features

Based on the Seahorse assay (illustrated in Supplementary Figure S1), five mitochondrial respiration-related bioenergetic features (basal respiration, ATP production, proton leak, maximal respiration and spare respiratory capacity) were calculated from the oxygen consumption rate (OCR) time course during a mitochondrial stress test (MST), and three glycolysis-related features (glycolysis, glycolytic capacity and glycolytic reserve) were calculated from the extracellular acidification rate (ECAR) during a glycolysis stress test (GST). The stress tests employ metabolically interfering compounds as described in the Supplementary Methods. In addition, the baseline OCR and ECAR values and the ECAR/OCR values were also defined as bioenergetic features.

1.4 Multi-omics profiling and ex-vivo drug sensitivity assay

Multi-omics profiling, including whole-exome sequencing, targeted sequencing, DNA methylation profiling and RNA sequencing, were previously performed on the same set of patient samples; in addition, the sensitivities of these samples to a panel of 63 small molecule compounds at 5 concentrations each were characterized [2]. Clinical outcomes of those sample were also recorded. Those data are available in the R data package BloodCancerMultiOmics2017, from the Bioconductor project (`http://bioconductor.org`).

1.5 Gene enrichment analysis

For the $n = 120$ patient samples for which we had both bioenergetic data and RNASeq data, the RNAseq data were used for identifying expression signatures of IGHV mutation status and for defining biological meanings of gene expression principal components selected by multivariate regression models. To characterize expression signatures of IGHV status, differentially expressed genes (FDR = 10%, method of Benjamini and Hochberg) were firstly identified by using DESeq2 [3] and then raked by their test statistics. As for defining the biological meanings of gene expression principal component, genes were ranked by their loadings on each principal components. Gene set enrichment analysis was then performed on the ranked lists using the Parametric Analysis of Gene Set Enrichment (PAGE) method [4] with the KEGG and H gene set selections from the MSigDB database (`http://software.broadinstitute.org/gsea/msigdb`).

1.6 Penalized multivariate regression

We performed multivariate regression to explain bioenergetic features by a large feature data space. We used a Gaussian linear model with L1-penalty (i.e., lasso regression) as implemented

in the R package glmnet version 2.0 with mixing parameter $\alpha = 1$ [5]. Before analysis the expression data were normalized and transformed using the *varianceStabilizingTransformation* function from DESeq2, and both expression and methylation data were filtered to include only the top 5000 most variable features each. Genetic mutations were only included in the model if present in at least 5 samples. Features with more than 20% missing values were excluded. Remaining missing values were imputed by the mean for methylation data and by the most common mutation status for genetic data.

As predictors in the lasso model the genetic mutations and IGHV status (coded as 0-1), demographics (age, sex) and the top 20 principal components of gene expression and methylation data were used. All features were scaled to unit variance and mean zero before using lasso to achieve fair treatment of all predictors by the penalty constraint. To compare explanatory power of different datasets a separate model was fit including only predictors of one omic type at a time as well as a joint model including all predictors. Using 3-fold cross-validation, the optimal penalty parameter λ was chosen to minimize the cross-validated R^2 of the model using the function *cv.glmnet*. The cross-validation process was repeated 100 times for each model to reduce the model variance, and then the average coefficient and feature selection frequency over 100 repeats were calculated. As a measure of explained variance, the reduction in cross-validated mean squared error relative to the null model was calculated and then averaged over 100 repeats. For single features, i.e. IGHV the R^2 from a standard linear model was used as corresponding quantity.

2 Supplementary Figures

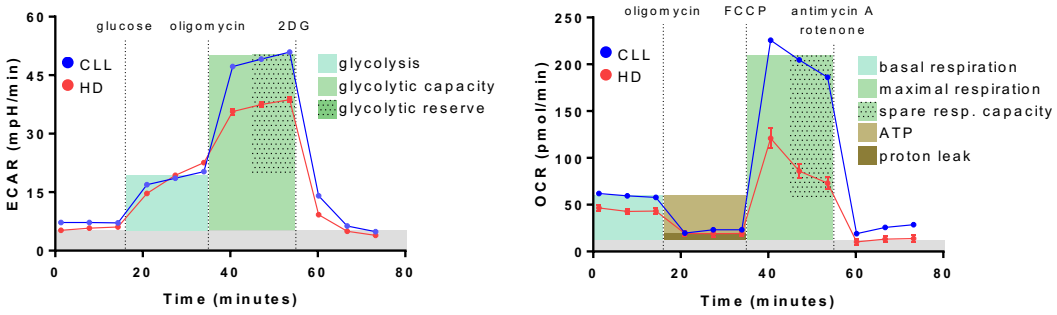

Figure S1: Representative scheme of the glycolytic stress test (left panel) and the mitochondrial stress test (right panel) depicting the extracellular acidification rate (ECAR) and the oxygen consumption rate (OCR), respectively. The calculation of the different metabolic parameters after sequential injection of metabolically active compounds is illustrated by colored boxes as indicated. The grey box symbolizes non-glycolytic acidification as well as non-mitochondrial respiration as background.

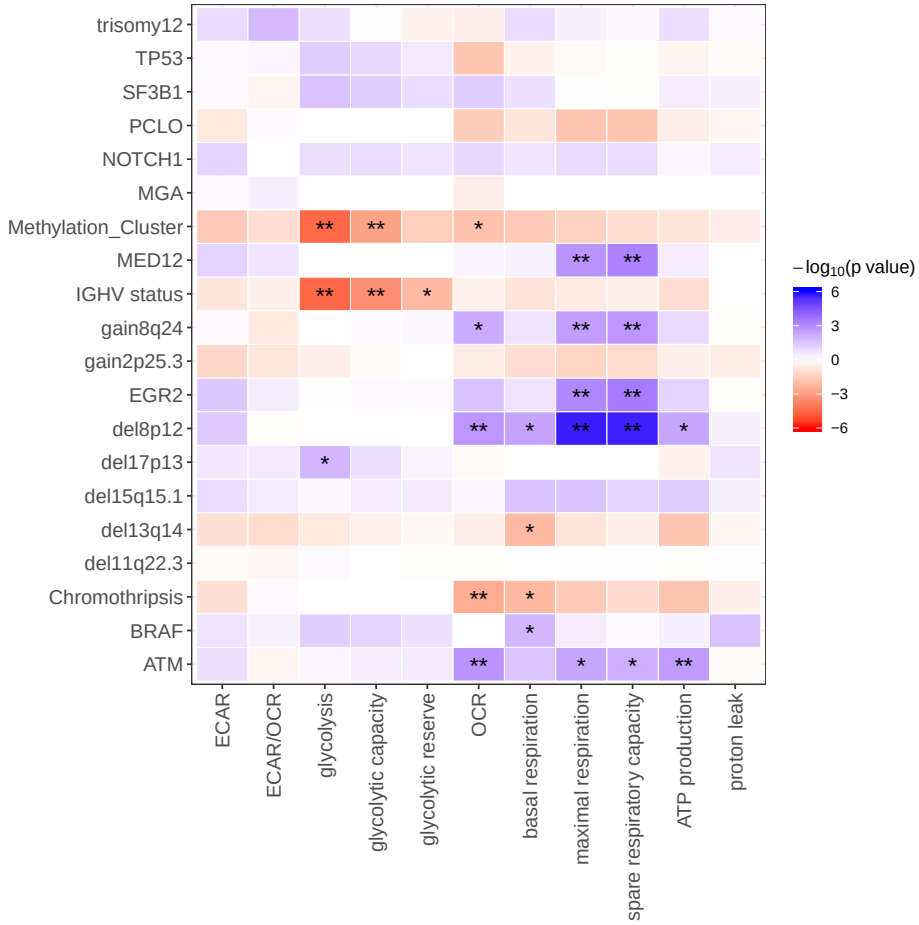

Figure S2: **A heatmap plot showing the p values for all tested associations between bioenergetic features and genetic variants.** A positive p value (colored by blue) indicates higher bioenergetic value in mutated cases (or highly methylated group for methylation cluster). A negative p value (colored by red) indicates lower bioenergetic value in mutated cases. ** indicates the association passed 5% FDR control and * indicates the association passed 10% FDR control, using the method of Benjamin and Hochberg on the set of 220 (20×11) raw p-values.

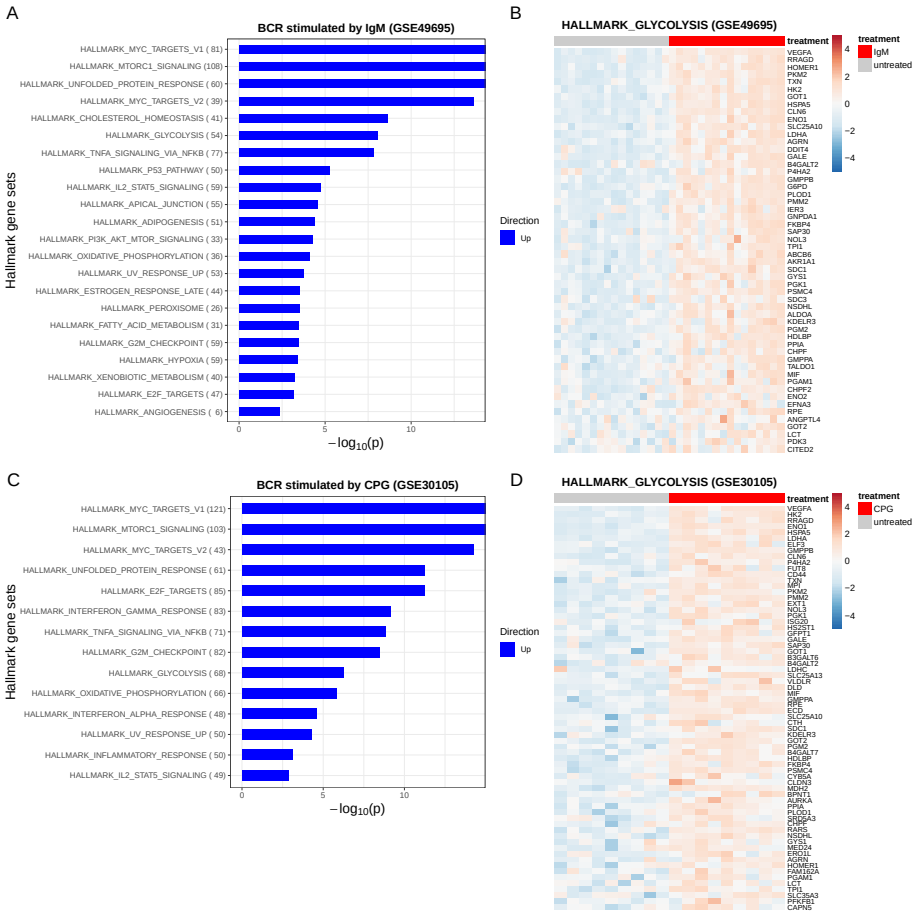

Figure S3: **Gene expression signatures of B-cell receptor stimulation queried from two public datasets** (A, C) *Hallmark* gene sets that are significantly enriched (method of Benjamini and Hochberg for FDR = 1%) among genes differentially expressed after BCR stimulation by IgM (GEO accession ID: GSE49695) or by CPG (GEO accession ID: GSE30105). (B,D) The heatmaps show the z-score of the expression values of glycolysis pathway genes that are differentially expressed after BCR stimulation by IgM or CPG.

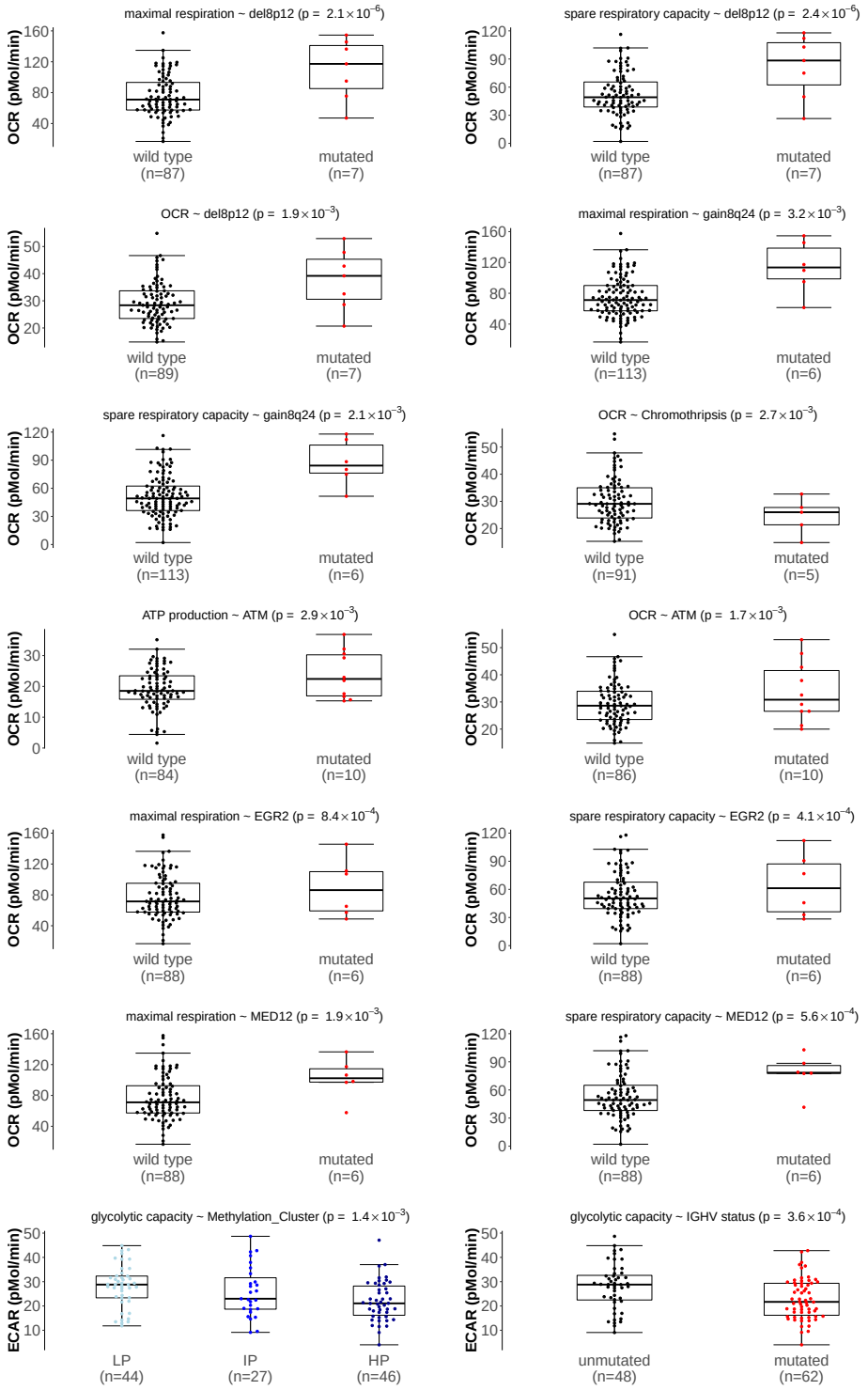

Figure S4: Beeswarm plots for all significant associations (method of Benjamini and Hochberg for FDR = 5%) between genetic variants and energy bioenergetic features

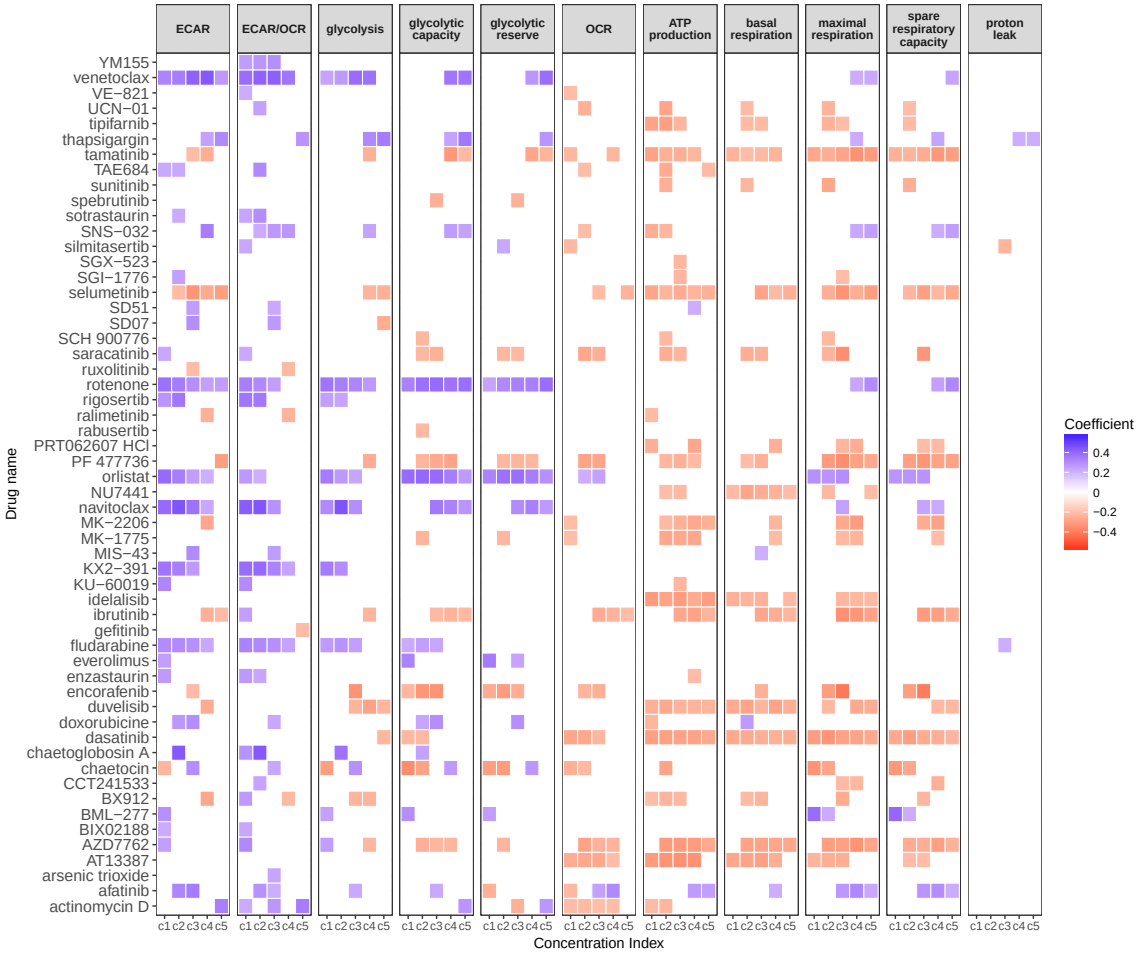

Figure S5: Correlations between bioenergetic features and drug response for all drug concentrations. Only the correlations passed 10% FDR threshold are shown. c1 indicates the highest concentration and c5 indicates the lowest concentration.

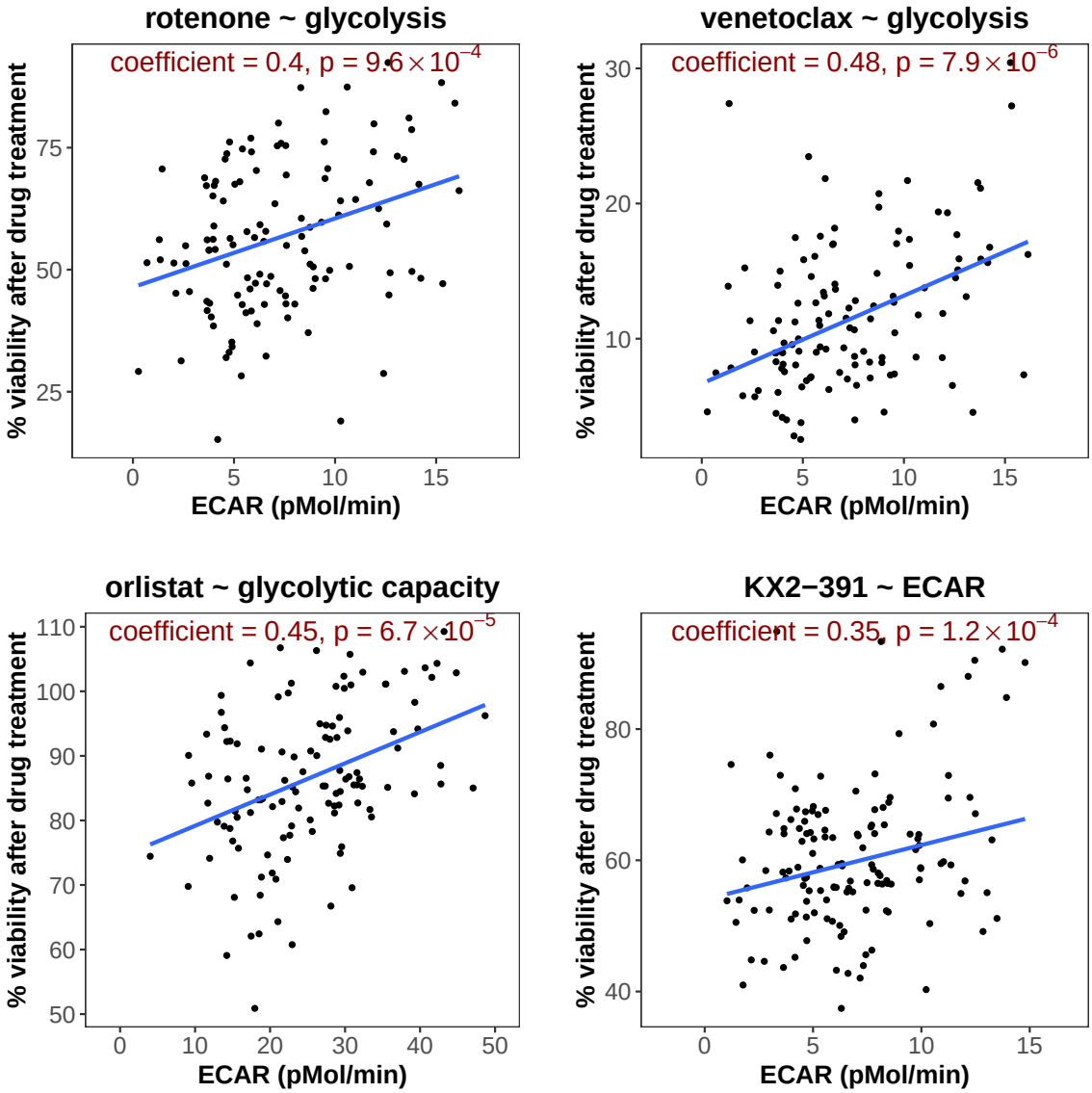

Figure S6: Exemplary scatter plots of the significant correlations between glycolysis-related features and drugs that target mitochondria. The x-axis shows the values of measured bioenergetic features, the y-axis shows the viabilities of the CLL samples after drug treatment.

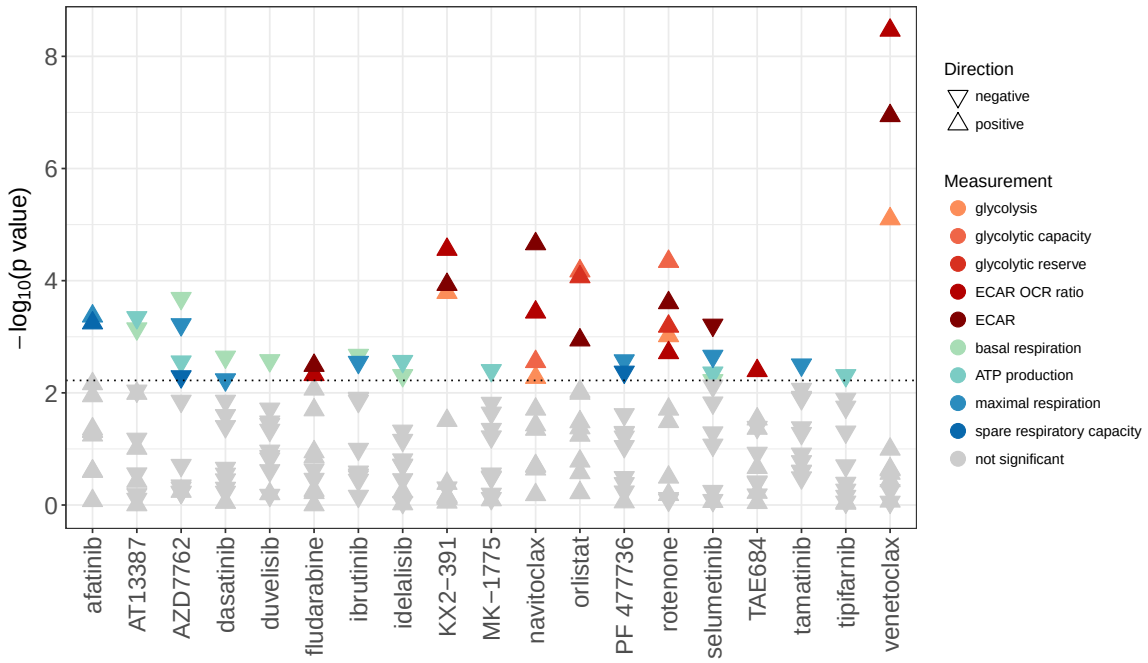

Figure S7: Correlation test results between drug response phenotype and bioenergetic features. Similar to main text Figure 4A, but IGHV status was included as a cofactor in a multivariate model in order to exclude the confounding effect of IGHV stauts. The dashed line indicate 5% FDR. The associations between glycolysis-related features and drugs such as venetoclax, navitoclax, rotenone, orlistat and KX2-391 are still significant in the multi-variate model, indicating the increased resistance to those drugs in CLL samples with higher glycolysis activity is not confounded by IGHV status.

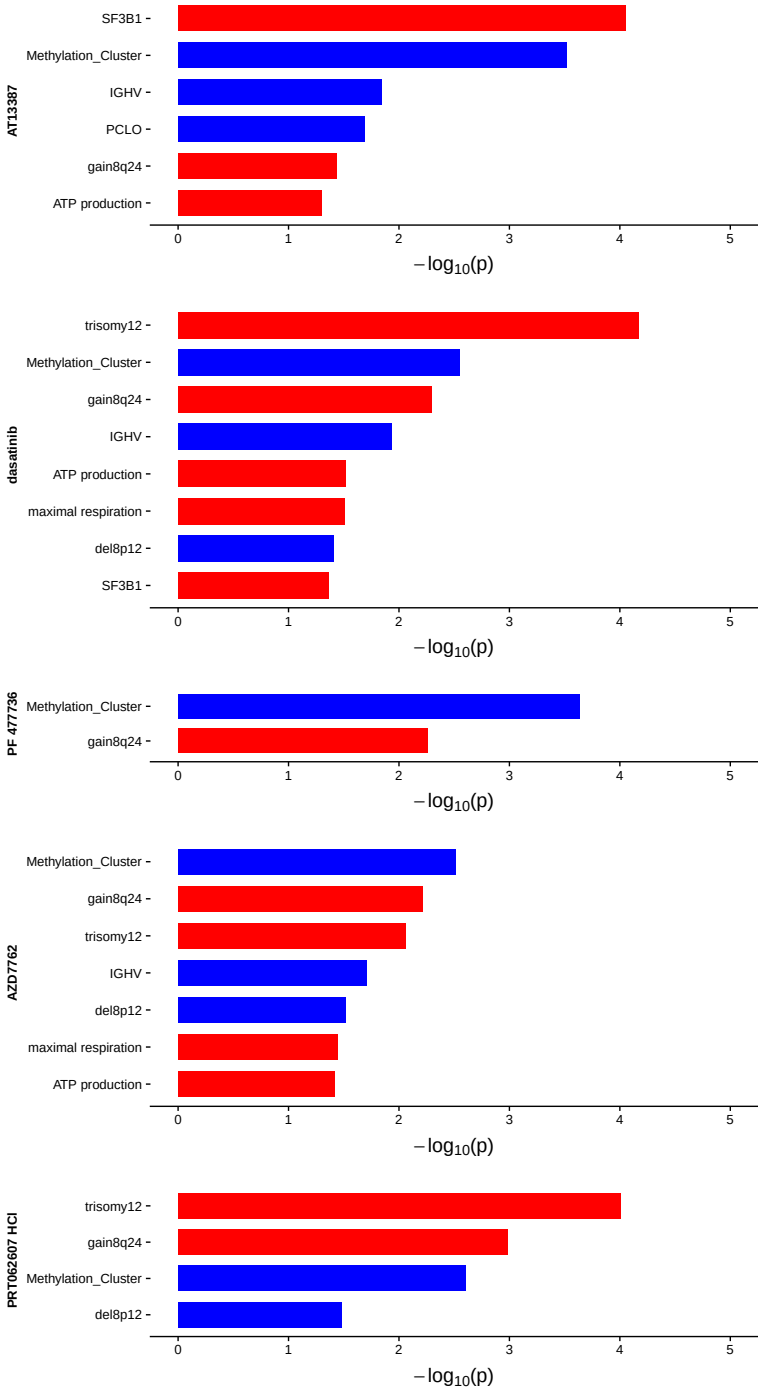

Figure S8: Drugs whose variance in patients responses can be well explained by genetic variants alone (drugs colored by blue in main text Figure 4B). The bar plots show the log_{10}(p value) of the corresponding feature. Red indicates a positive association with drug responses (higher drug sensitivity associates to mutation or higher bioenergetic feature value) while blue indicates a negative association with drug responses (higher drug resistance associates to mutation or higher bioenergetic feature value). Only the features with p values less than 0.05 in the multivariate linear regression models are shown.

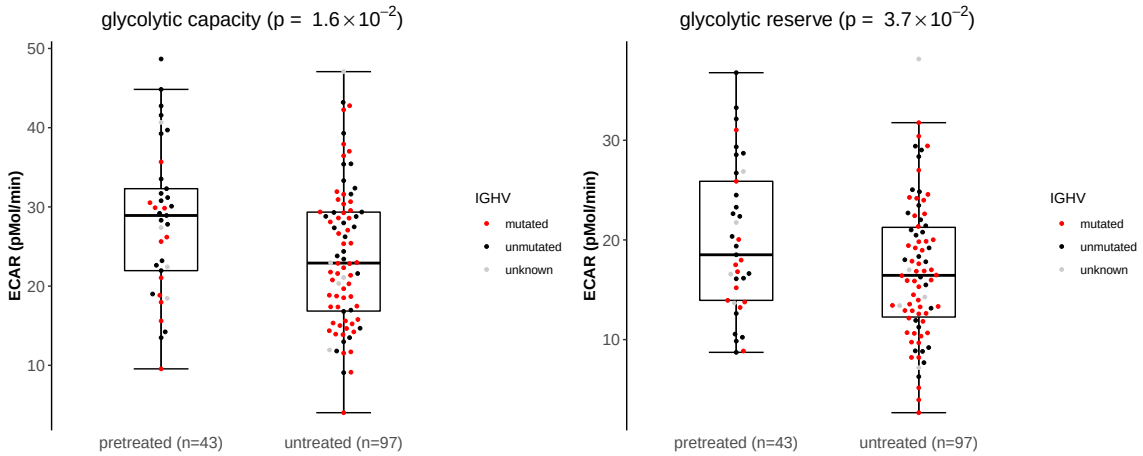

Figure S9: Beeswarm plots for associations of pretreatment status with glycolytic capacity (A) and glycolytic reserve (B).

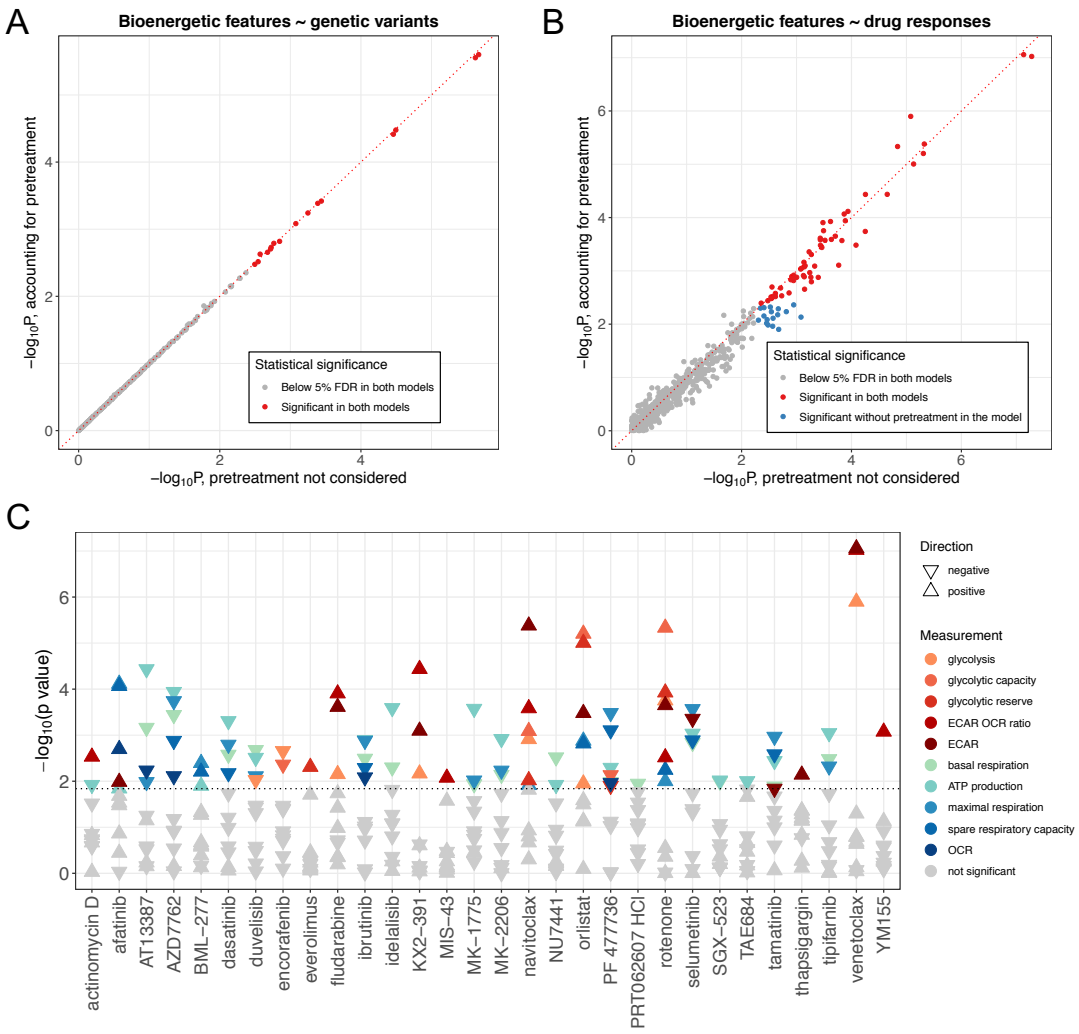

Figure S10: **Impact of pretreatment status on the associations of bioenergetic features to genetic variants and drug responses.** (A,B) Comparison of p values between the model without considering pretreatment status and the model considering pretreatment status. The scatter plot indicates that the test results from the two models are highly concordant. (C) Correlation test results between drug response phenotype and bioenergetic features. Similar to main text Figure 4A, but pretreatment status was included as a cofactor in a multivariate model in order to exclude the confounding effect of pretreatment stauts. The dashed line indicate 5% FDR. The two plots are highly similar, suggesting a very minimal impact of pretreatment status on the association between bioenergetic features and drug responses.

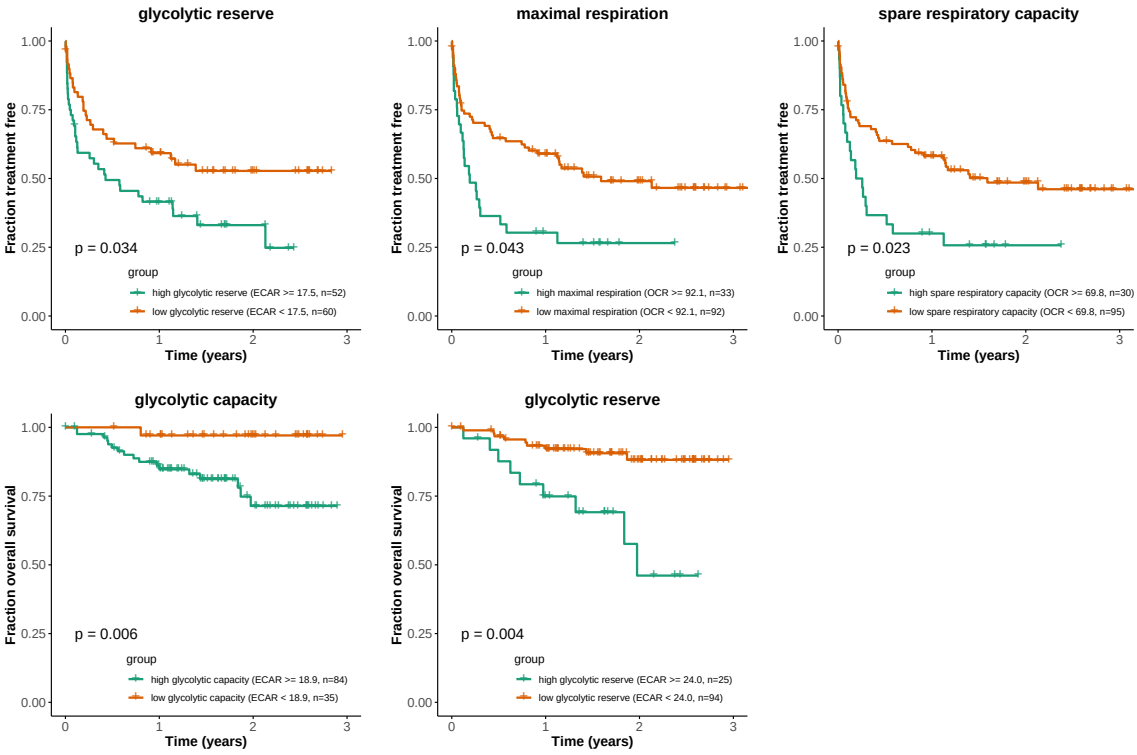

Figure S11: Kaplan-Meier plots for overall survival (OS) and time to treatment (TTT) stratified by bioenergetic features. P-values were calculated from univariate Cox regression with bioenergetic features treated as continuous variables. To visualize the effect using Kaplan-Meier plots, the patients were categorized into two groups, with high and low energy metabolic activity, using maximally selected rank statistics as cut-offs. The cutoff value and number of samples in each group are shown inside the parentheses in the figure legends.

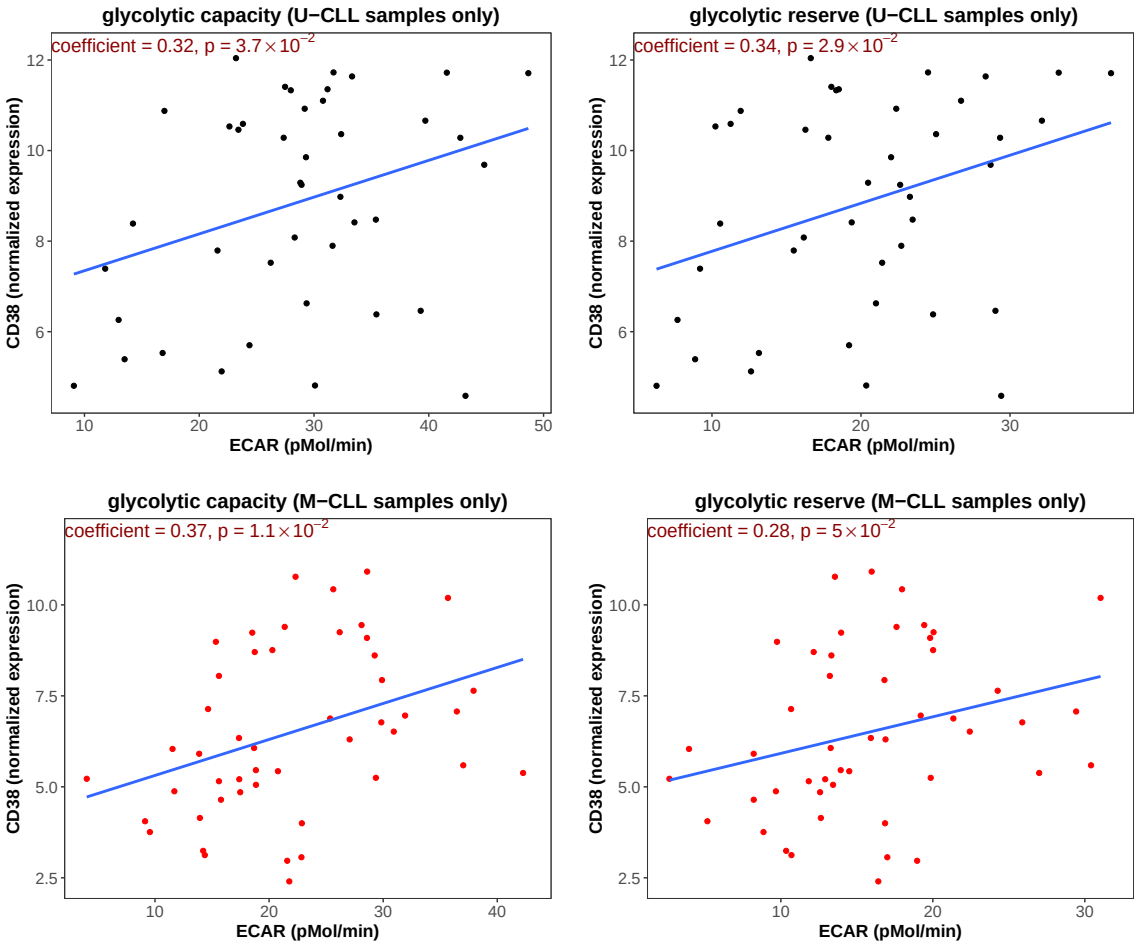

Figure S12: Scatter plots for associations of CD38 expression with glycolytic capacity and glycolytic reserve in U-CLL samples and M-CLL samples separately.

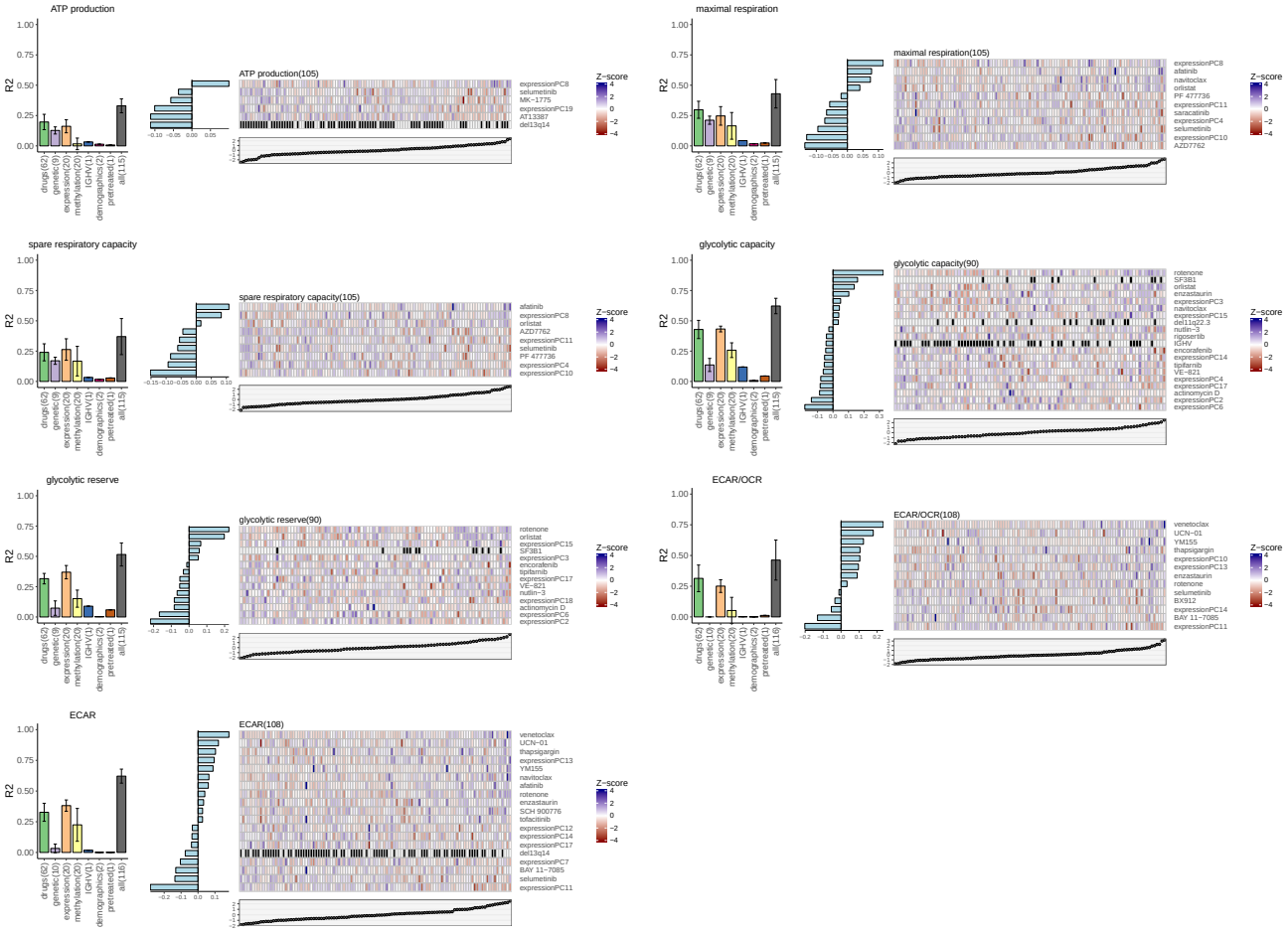

Figure S13: Barplots for explanatory power (R2) of features from different data types for the prediction of energy metabolism and visualization of fitted adaptive LASSO regularization multivariate models, for bioenergetic features not shown in main text Figure 6.

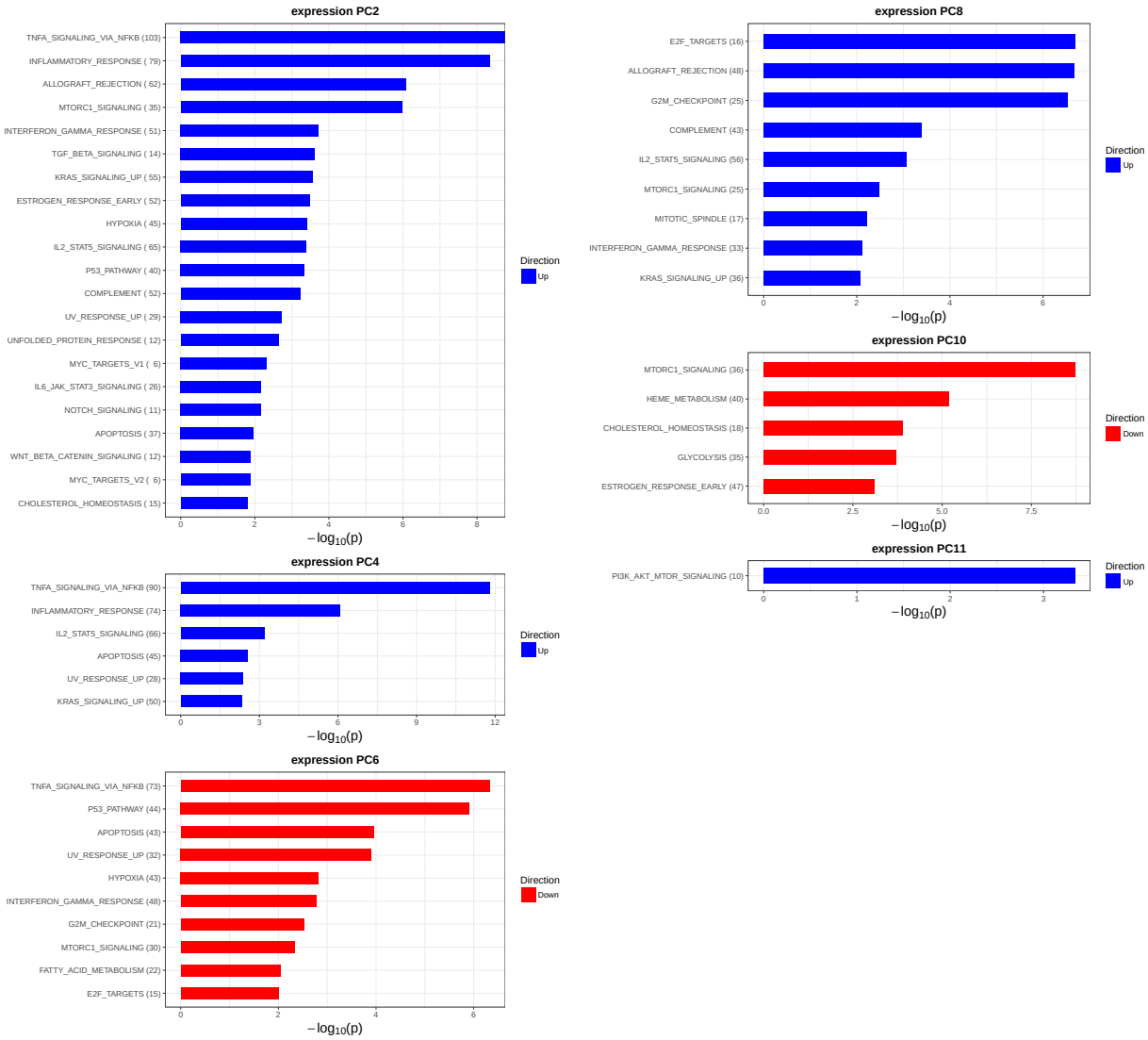

Figure S14: Gene set enrichment analysis on the genes correlated with principal components that are frequently picked by multivariate models as predictors for energy metabolism phenotype.

3 Supplementary Tables

Table S1: Background information of patients included in the study. (n.d. - no data available)

No.	Patient ID	Sex	IGHV	Age	Methylation_Cluster	Pretreated	Type of treatment
1	H017	m	U	56	LP	no	
2	H015	f	U	62	LP	no	
3	H023	f	U	70	LP	yes	Chemoimmunotherapy
4	H033	f	M	62	HP	no	
5	H035	f	M	79	IP	yes	Chemoimmunotherapy
6	H036	f	M	75	HP	no	
7	H040	f	M	83	IP	no	
8	H042	f	U	71	LP	yes	Chemoimmunotherapy
9	H046	m	M	88	HP	no	
10	H014	f	U	86	LP	yes	Chemoimmunotherapy
11	H028	f	M	72	HP	no	
12	H062	m	M	53	n.d.	no	
13	H065	f	U	77	LP	yes	Chemoimmunotherapy
14	H010	f	U	72	LP	no	
15	H027	m	U	57	LP	no	
16	H069	f	U	76	LP	yes	Chemoimmunotherapy
17	H063	f	M	49	IP	no	
18	H082	m	M	82	IP	no	
19	H072	m	U	57	IP	no	
20	H056	m	M	83	HP	no	
21	H021	m	M	49	HP	no	
22	H011	f	M	72	HP	no	
23	H078	m	U	68	LP	yes	Chemoimmunotherapy
24	H012	f	U	61	LP	yes	Chemoimmunotherapy
25	H016	m	M	55	IP	no	
26	H057	m	M	66	HP	no	
27	H045	m	U	90	LP	yes	Chemoimmunotherapy
28	H013	m	U	77	LP	yes	Chemoimmunotherapy
29	H094	m	M	45	HP	no	
30	H060	m	U	75	HP	no	
31	H039	f	M	54	HP	no	
32	H090	f	M	70	IP	yes	Chemoimmunotherapy
33	H095	f	U	52	LP	no	
34	H029	f	M	75	IP	yes	Chemoimmunotherapy
35	H020	m	M	64	HP	no	
36	H019	f	U	70	IP	yes	Chemoimmunotherapy
37	H041	m	M	75	HP	no	
38	H100	m	M	74	HP	no	
39	H032	m	U	67	LP	yes	Chemoimmunotherapy
40	H101	f	M	72	HP	no	
41	H102	f	U	78	LP	no	
42	H044	m	U	59	IP	yes	Chemoimmunotherapy
43	H083	m	n.d.	69	HP	no	
44	H104	m	U	79	LP	no	
45	H058	f	M	74	IP	no	
46	H077	f	U	69	LP	no	
47	H031	f	M	62	IP	no	
48	H005	m	M	75	IP	yes	Chemoimmunotherapy
49	H105	m	M	49	HP	no	
50	H081	f	M	64	HP	no	
51	H106	m	M	70	HP	no	
52	H054	f	M	49	HP	no	
53	H089	f	M	54	HP	no	

54	H108	m	M	57	HP	no	
55	H047	m	U	68	LP	yes	Chemoimmunotherapy
56	H064	m	n.d.	71	LP	yes	Chemoimmunotherapy
57	H113	m	M	69	IP	no	
58	H066	m	U	47	LP	yes	Chemoimmunotherapy
59	H111	m	U	54	LP	yes	Chemoimmunotherapy
60	H043	f	U	44	LP	yes	Chemoimmunotherapy
61	H088	f	M	59	HP	no	
62	H107	m	U	43	LP	no	
63	H051	f	U	78	IP	yes	Chemoimmunotherapy
64	H118	m	M	49	IP	yes	Chemoimmunotherapy
65	H093	f	U	76	LP	no	
66	H030	m	U	52	LP	no	
67	H053	f	M	83	IP	no	
68	H059	m	M	54	HP	no	
69	H096	f	n.d.	61	HP	no	
70	H080	m	U	81	LP	yes	Chemoimmunotherapy
71	H133	m	n.d.	68	HP	no	
72	H073	m	M	64	IP	yes	Chemoimmunotherapy
73	H135	f	M	76	HP	yes	Chemoimmunotherapy
74	H079	m	U	47	LP	no	
75	H136	m	U	65	LP	yes	Chemoimmunotherapy
76	H103	m	M	70	IP	no	
77	H148	f	U	33	LP	yes	Chemoimmunotherapy
78	H164	f	U	73	LP	no	
79	H165	f	U	57	LP	no	
80	H166	f	U	62	LP	no	
81	H099	f	M	54	HP	no	
82	H115	m	M	72	IP	no	
83	H037	m	M	71	IP	no	
84	H067	f	M	77	HP	no	
85	H169	f	M	41	HP	no	
86	H170	f	M	74	HP	yes	Chemoimmunotherapy
87	H184	m	M	74	HP	no	
88	H084	m	M	87	LP	no	
89	H186	f	M	72	IP	no	
90	H070	m	n.d.	71	HP	no	
91	H171	m	U	73	LP	yes	Chemoimmunotherapy
92	H173	f	M	73	IP	yes	Chemoimmunotherapy
93	H228	m	U	64	IP	no	
94	H229	f	M	74	n.d.	yes	Chemoimmunotherapy
95	H191	m	n.d.	38	IP	yes	Chemoimmunotherapy
96	H230	m	U	70	IP	yes	Chemoimmunotherapy
97	H055	m	M	64	HP	no	
98	H168	m	n.d.	57	IP	yes	Chemoimmunotherapy
99	H192	f	M	72	IP	no	
100	H185	f	M	86	HP	no	
101	H187	m	U	59	LP	no	
102	H109	m	U	85	LP	no	
103	H049	m	M	58	IP	no	
104	H163	m	M	65	HP	no	
105	H231	m	U	46	LP	no	
106	H234	m	U	68	LP	no	
107	H235	m	M	73	HP	no	
108	H236	m	M	67	HP	no	
109	H225	f	M	46	HP	no	
110	H038	m	M	73	HP	no	
111	H237	f	M	73	IP	no	

112	H238	m	U	74	LP	no	
113	H240	m	M	82	IP	no	
114	H233	m	U	54	LP	no	
115	H242	m	U	48	LP	no	
116	H243	m	U	79	LP	no	
117	H167	f	U	64	LP	no	
118	H247	f	M	46	HP	no	
119	H194	m	M	75	HP	no	
120	H248	f	M	62	HP	no	
121	H050	f	M	62	n.d.	no	
122	H246	m	U	74	LP	no	
123	H249	m	U	83	LP	no	
124	H137	m	M	53	HP	no	
125	H110	m	M	66	HP	no	
126	H252	m	U	69	LP	no	
127	H255	m	U	67	LP	yes	Chemoimmunotherapy
128	H239	f	U	69	LP	no	
129	H256	f	n.d.	62	HP	yes	Chemoimmunotherapy
130	H257	f	U	65	LP	no	
131	H258	m	M	64	HP	no	
132	H259	m	U	60	LP	yes	Chemoimmunotherapy
133	H264	m	M	77	HP	yes	Chemoimmunotherapy
134	H265	m	U	59	LP	yes	Chemoimmunotherapy
135	H260	m	U	62	LP	yes	Chemoimmunotherapy
136	H268	m	n.d.	82	HP	no	
137	H266	m	M	74	HP	yes	Chemoimmunotherapy
138	H270	f	M	66	IP	no	
139	H271	m	M	65	HP	no	
140	H272	m	U	55	LP	yes	Chemoimmunotherapy

Table S2: ANOVA test results (adjusted for batch effect) of bioenergetic features between CLL cells and normal B cells

Seahorse measurement	p	Difference of mean	adjusted p
ATP production	0.000	15.333	0.000
basal respiration	0.000	16.308	0.000
ECAR	0.013	-2.890	0.016
ECAR/OCR	0.000	-0.622	0.000
glycolysis	0.972	-0.044	0.972
glycolytic capacity	0.000	13.896	0.000
glycolytic reserve	0.000	13.940	0.000
maximal respiration	0.000	58.044	0.000
OCR	0.000	17.166	0.000
proton leak	0.629	0.975	0.692
spare respiratory capacity	0.000	41.736	0.000

Table S3: Association test results of bioenergetic features related to pretreatment status

Seahorse mearuement	p value	adjusted p	p value (IGHV blocked)	adjusted p (IGHV blocked)
ATP production	0.755	0.831	0.867	0.934
basal respiration	0.641	0.821	0.934	0.934
ECAR	0.672	0.821	0.426	0.670
ECAR/OCR	0.245	0.385	0.271	0.597
glycolysis	0.065	0.185	0.229	0.597
glycolytic capacity	0.016	0.174	0.083	0.597
glycolytic reserve	0.037	0.185	0.114	0.597
maximal respiration	0.101	0.185	0.489	0.672
OCR	0.098	0.185	0.224	0.597
proton leak	0.851	0.851	0.925	0.934
spare respiratory capacity	0.085	0.185	0.409	0.670

Table S4: Multivariate Cox regression model for time to treatment with glycolytic reserve as a covariate

factor	p value	hazard ratio	lower 95% CI	upper 95% CI
age	0.0397	0.77	0.61	0.99
trisomy12	0.594	1.3	0.53	3.1
11q22.3 deletions	0.622	1.2	0.55	2.7
17p13 deletions	0.556	1.3	0.55	3
TP53 mutations	0.0125	2.6	1.2	5.6
U-CLL	0.108	1.8	0.88	3.6
glycolytic reserve	0.095	1	0.99	1.1

Table S5: Multivariate Cox regression model for time to treatment with maximal respiration as a covariate

factor	p value	hazard ratio	lower 95% CI	upper 95% CI
age	0.0169	0.77	0.62	0.95
trisomy12	0.336	1.5	0.66	3.3
11q22.3 deletions	0.18	1.6	0.79	3.4
17p13 deletions	0.581	1.3	0.54	3
TP53 mutations	0.00532	3	1.4	6.4
U-CLL	0.0354	2	1	3.8
maximal respiration	0.0743	1	1	1

Table S6: Multivariate Cox regression model for time to treatment with spare respiratory capacity as a covariate

factor	p value	hazard ratio	lower 95% CI	upper 95% CI
age	0.0191	0.77	0.62	0.96
trisomy12	0.328	1.5	0.67	3.4
11q22.3 deletions	0.187	1.6	0.79	3.4
17p13 deletions	0.572	1.3	0.54	3
TP53 mutations	0.00743	2.9	1.3	6.1
U-CLL	0.0332	2	1.1	3.8
spare respiratory capacity	0.0672	1	1	1

Table S7: Correlation tests between each Seahorse measurements and lymphocyte doubling time

Seahorse mearuement	p value	adjusted p	p value (IGHV blocked)	adjusted p (IGHV blocked)
ATP production	0.170	0.442	0.519	0.815
basal respiration	0.666	0.814	0.786	0.959
ECAR	0.838	0.862	0.435	0.815
ECAR/OCR	0.862	0.862	0.161	0.815
glycolysis	0.032	0.199	0.778	0.959
glycolytic capacity	0.036	0.199	0.488	0.815
glycolytic reserve	0.099	0.364	0.452	0.815
maximal respiration	0.505	0.729	0.959	0.959
OCR	0.201	0.442	0.143	0.815
proton leak	0.330	0.605	0.269	0.815
spare respiratory capacity	0.530	0.729	0.882	0.959

Table S8: Associations of bioenergetic features with CD38 and IGTA4(CD49d) expression

Measurement	Gene	p value	p value (IGHV blocked)	adjusted p value	adjusted p value (IGHV blocked)
glycolytic capacity	CD38	0.000	0.001	0.001	0.021
glycolytic reserve	CD38	0.000	0.003	0.003	0.033
glycolysis	CD38	0.001	0.019	0.004	0.083
maximal respiration	CD38	0.002	0.032	0.009	0.083
glycolysis	ITGA4	0.003	0.028	0.013	0.083
ECAR	CD38	0.005	0.009	0.015	0.067
spare respiratory capacity	CD38	0.005	0.072	0.015	0.121
basal respiration	ITGA4	0.005	0.028	0.015	0.083
basal respiration	CD38	0.006	0.027	0.015	0.083
OCR	CD38	0.009	0.070	0.021	0.121
ATP production	CD38	0.013	0.070	0.026	0.121

References

[1] Leek JT, Johnson WE, Parker HS, Jaffe AE, Storey JD. The sva package for removing batch effects and other unwanted variation in high-throughput experiments. Bioinformatics (Oxford, England). 2012 mar;28(6):882–3. Available from: http://www.ncbi.nlm.nih.gov/pubmed/22257669http://www.pubmedcentral.nih.gov/articlerender.fcgi?artid=PMC3307112.

[2] Dietrich S, Oleś M, Lu J, Sellner L, Anders S, Velten B, et al. Drug-perturbation-based stratification of blood cancer. The Journal of clinical investigation. 2017 dec;128(1). Available from: https://www.jci.org/articles/view/93801http://www.ncbi.nlm.nih.gov/pubmed/29227286.

[3] Love MI, Huber W, Anders S. Moderated estimation of fold change and dispersion for RNA-seq data with DESeq2. Genome Biology. 2014 dec;15(12):550. Available from: http://genomebiology.biomedcentral.com/articles/10.1186/s13059-014-0550-8.

[4] Kim SY, Volsky DJ. PAGE: parametric analysis of gene set enrichment. BMC bioinformatics. 2005 jun;6:144. Available from: http://www.ncbi.nlm.nih.gov/pubmed/15941488http://www.pubmedcentral.nih.gov/articlerender.fcgi?artid=PMC1183189.

[5] Friedman J, Hastie T, Tibshirani R. Regularization Paths for Generalized Linear Models via Coordinate Descent. Journal of Statistical Software. 2010 feb;33(1):1–22. Available from: http://www.jstatsoft.org/v33/i01/.